MECHANICAL ASPECTS OF THE DESIGN OF THIRD-GENERATION SYNCHROTRON-LIGHT SOURCES

S. Zelenika
Paul Scherrer Institute, Villigen, Switzerland

Abstract
In storage rings of third-generation synchrotron radiation facilities, the positioning tolerances of the elements of the machine are constantly reduced to achieve lower emittance and increased lifetime. This implies increasing positioning and alignment precision that must be preserved over long time-spans. The mechanical engineering approach to meet these requirements is described. The design of the Swiss Light Source storage ring support, positioning and position monitoring systems, the tests done on the respective prototypes, the quality assurance and installation procedures, and the operational experience with these systems are discussed in depth. The applicability of the developed arrangement to beam-based alignment is also illustrated.

1 Introduction

In the design of third-generation synchrotron-light sources and related experimental infrastructure, there is a wide range of mechanical engineering tasks to satisfy. Therefore, the mechanical engineering crew is confronted with several topics related to these designs [1–3]:

- ultra-high-precision positioning of optical and other elements with resolutions, accuracies and precisions in the nanometric and μrad ranges;

- high-precision machining with tolerances of the produced pieces of equipment in the micrometre range;

- vibration measurement and suppression, with maximum allowed vibration amplitudes often limited to the nanometre range;

- high-heat-load problems, with pieces of equipment subject to specific heat loads approaching 1 GW/m^2 [4, 5], i.e., considerably higher than those on the surface of the sun where $7{\times}10^7$ W/m^2 are reached;

- high and ultra-high vacuum issues (with the respective limits imposed, for example, on the use of materials or types of positioning mechanisms), where the ultimate pressures reached are in the low 10^{-10} mbar range;

- radiation compatibility, with stringent limits on the available selection of materials and components used;

- experimental technologies pertaining to all of the above fields;

- innovative, analytical and numerical methods needed to satisfy the technical challenges cited;

- use of advanced computer-aided engineering systems [computer-aided design (CAD) and manufacturing (CAM), finite-element methods (FEM), database management tools, etc.].

In the design of synchrotron accelerator complexes, increasing attention is dedicated to the proper mechanical design of the storage ring support, positioning and position monitoring systems. The sources of beam instabilities causing orbit distortions, and the effects generated by ground motion

(ground settlement, seasonal changes, and temperature effects) and by dynamic excitation sources (local machinery, water cooling, and near-by roads) have to be minimized [5–8] to attain the required beam quality (high brightness, i.e. low emittance) and lifetimes.

Fig. 1: View of the interior of the SLS building during its construction

In this paper an approach to deal effectively with these challenges is illustrated using the example of the mechanical design of the Swiss Light Source (SLS) machine (Fig. 1) at the Paul Scherrer Institute (PSI, Villigen, Switzerland). SLS is the first medium-energy-range synchrotron facility of hard X-rays that uses the higher spectral harmonics of in-vacuum undulators with a short period and a small gap. The main goal at the SLS was to achieve a very high photon-beam quality, which is, in turn, determined by the electron-beam quality. Since the remaining space for the optimization of the lattices is limited, the positioning, re-positioning and alignment precision of the magnets by mechanical means were considered extremely important to attain the low emittances required and to reduce orbit distortions before switching on the correction dipoles [9]. Hence, in order to meet the high-quality requirements, provisions for accurate positioning, as well as dynamic minimization of ground motions and thermal effects, were foreseen from the very beginning of the SLS storage ring design.

2   Aims of the work

Considering these arguments, the mechanical design goals for the SLS storage ring support, alignment and disturbances compensation systems are to

- support the storage ring magnets, vacuum chambers, diagnostics devices and position measurement systems (horizontal positioning system—HPS, and hydrostatic levelling system—HLS);

- obtain one large, rigid, pre-assembled item not necessitating fiducialization of individual magnets or items other than the support itself;

- provide high-precision reference surfaces for the magnets both in the horizontal and in the vertical direction (out of the total alignment tolerances, only 30 µm are 'at disposal' for the manufacturing tolerances of the supports);

- provide a simple and reliable mechanical design allowing easy mounting and alignment;

- provide a kinematic support (number of constrains balances the number of the needed degrees of freedom—DOFs);

- provide means of compensating for thermal and geological horizontal and vertical disturbances with large time constants;

- provide smooth, hysteresis-free and remotely controllable motion at micrometric levels;

- guarantee the stiffness (dynamic stability) of the support structures with magnets mounted onto them such that the residual r.m.s. beam jitter—including optics amplification—remains smaller than 10% of the r.m.s. beam sigmas (i.e., considering a 1% emittance coupling, the jitter should not exceed 1 μm vertically and 10 μm horizontally) [10].

3   Basic design

3.1   Support system

Various solutions have been adopted at synchrotron light and other accelerator facilities around the world to support the elements of the machine [11]. The individual support stands are generally used when the accelerator components are spread out, while girders are the preferred solution when a set of components has to be mounted on a common platform. The latter solution avoids the ground settlement of individual components, permits the vacuum chambers to be supported on the same structure thus guaranteeing the tolerances needed between the magnets and the vacuum system, and the girders can be pre-assembled. Moreover, as shown below, random displacements of girders with several magnets mounted onto them generate a lesser impact on orbit distortion than do individually supported quadrupoles.

Given that these advantages, fulfil the requirements perfectly, a girder-based support system was adopted in the SLS case. The cross section of the girders was then determined based on the optimization of their mechanical characteristics, with the intention of minimizing the cross sectional area (which is directly proportional to the costs and the mass of the structure), while concurrently maximizing the stiffness of the girders. It can be shown [12] that for bending loads the optimal shape to meet these goals is either an 'I' or a hollow-square-cross-section. In the case of torsion loads, the optimum is reached with closed hollow shapes, possibly with ribs along the length of the structure.

Based on these considerations, a welded, stress-relieved (annealed), hollow-square girder structure with internal ribs was adopted as the basic support unit of the SLS storage ring elements (Fig. 2). The girder design included an extensive optimization process based on the numerical sensitivity analysis of the main design parameters (such as longitudinal distance between the support points, their vertical position relative to the centre of mass of the girder/magnet assembly, wall thickness of the girder structure) so as to maximize the static and dynamic stiffness of the girder assemblies [13].
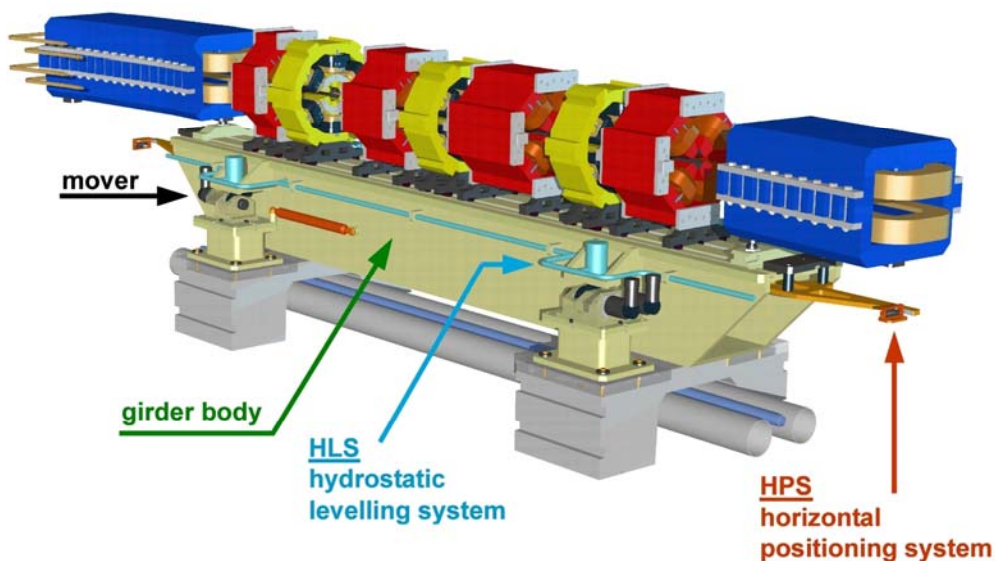

Fig. 2: The SLS storage ring support, alignment and disturbances compensation systems

In total, 48 girders are used of which 30 are 4.5 m in length and 18 are 3.7 m in length. Four girders are placed in each of the 12 triple-bend achromats (TBAs—four TBAs then form one superperiod containing a 11.8 m, a 7 m, and two 4 m long straight sections) of the SLS storage ring. The upper part of the girders is designed to provide ground horizontal and vertical reference surfaces with a precision of $\leq \pm 15$ µm (Fig. 3) onto which the magnets (whose reference surfaces were also given narrow tolerances so as to achieve the global goal of keeping the total mechanical tolerances to within ± 50 µm) are laid and fixed via suitably designed clamps.
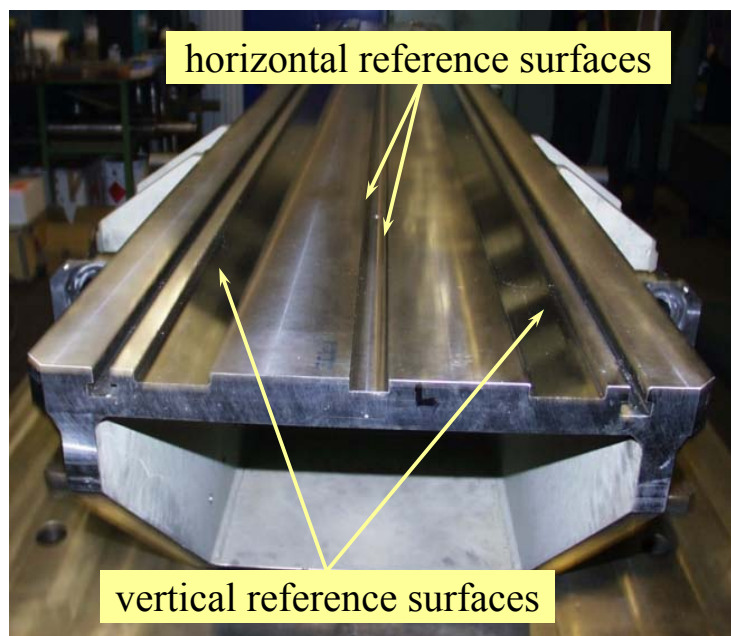

Fig. 3: Reference planes for positioning the storage ring elements on the girders

Kinematically supported dipole magnets (the conventional flat-V-cone kinematic mount balances the six DOFs) overlap adjacent girders establishing, together with the HPS foreseen and HLS systems (see below), a virtual 'train link' scheme with joints near the centres of the dipoles.

Continuous monitoring and correction of girder location is required to compensate for girder misalignment relative to the ideal position due to geological and thermal drifts, and to guarantee sufficient dynamic apertures.

3.2   Positioning system

Alignment and disturbance compensation targets have also been met at various accelerator facilities using different approaches [11]. At the European Organization for Nuclear Research (CERN), the Stanford Linear Accelerator Center (SLAC) and the Deutsches Elektronen-Synchrotron (DESY), the positioning in the horizontal and vertical plane is separate. The vertical system, based on shim stacks, threaded rods, wedge jacks or screw jacks is constituted by three standoffs allowing the heave, the roll and the pitch to be adjusted. The horizontal system constitutes one or two sliding plates with a push–push screw or a turnbuckle push–pull rail-slide-based system. Obviously in this case the alignment procedure is iterative, often leading to a coupled motion in more DOFs, thus resulting in considerable time loss.

Therefore, at the Advanced Light Source (ALS), the 'six-strut system' constituted by length-adjustable bars with spherical joints at the ends has been developed. Three of the bars are used for the adjustment in the vertical plane (heave, roll and pitch), while the remaining three lie in the horizontal plane and are used to adjust the sway, surge and jaw of the structure under consideration. However, the six-strut system still presents the disadvantages of rather limited load capacity, residual coupling of

the DOFs because of the cosine effect, intermittent motion due to stick-slip effects at the strut fixations, as well as several sources of backlash all leading to reduced accuracy.

A motorized Kelvin clamp-based kinematic positioning system was recently developed at SLAC [14]. The positioning is obtained via eccentric cam-shaft support drives ('movers') driven via stepping motors, with a linear variable differential transformer (LVDT)-based feedback system. The system allows simultaneous remotely controllable multi-DOF movements to be performed, while minimizing friction and hysteresis by substituting conventional sliding with pure rolling motions (only the inner eccentric shaft rotates, while the outer part of the cam remains in contact with the girder body). As a result, the required smooth incremental motions can be obtained using conventional (low-cost) mechanical components. In the proposed configuration, however, the range of motion of the system was limited to ±2 mm, while the loading capacity was limited to roughly 1 ton.

Based on these experiences, SLS adopted a pre-alignment, push–push, screw arrangement mounted on the four pedestals underneath each girder, and for the final micrometric-range alignment, the mover system (Fig. 4). However, several design modifications have been introduced to the original SLAC mover design:

- the range of motions of the movers was increased to ±5 mm to suit SLS needs;

- costly stepping motors were replaced by simple d.c. motors;

- in the feedback loop the LVDTs were replaced by absolute rotary encoders, avoiding the necessity of lengthy LVDT mounting and calibration procedures [14];

- instead of ball bearings, commercially available (SKF) spherical roller bearings were press-fitted onto the precisely machined cam-shafts, thus providing means for adaptation to small misalignments between the bearings and the respective seats on the girders, but also, given the larger contact area, increasing the load-carrying capacity (the SLS girder-magnet assembly weighs up to 9 tons) and stiffness.
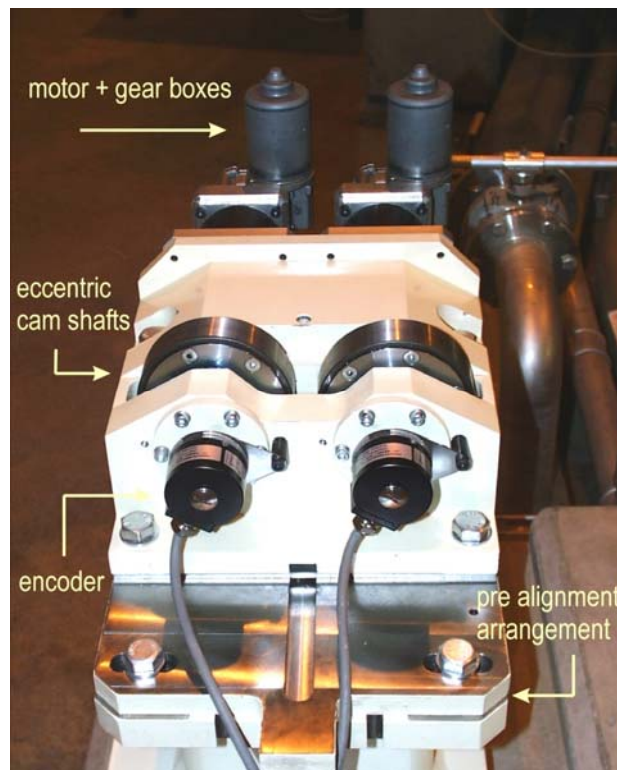

Fig. 4: Mover system

The envisaged positioning system fulfils the design goals, while the overall kinematicity of the support (Fig. 5) concurrently enables the following advantages [15]:

- a self-locating feature, free from backlash, permits alignment and possible repeat re-positioning in the micrometric and even sub-micrometric range;

- the probability of foreign matter contaminating the interface and reducing repeatability is reduced (particles or films on the points of contact will very likely be squeezed out by the high contact pressures at the interface);

- since the support is not overconstrained, it is deterministic, i.e., its behaviour can be represented in a closed form solution;

- no clamping forces other than gravity can distort the girder shape (no overconstraining induced stresses are present);

- the support allows for thermal expansions, keeping the resulting mechanical stresses to a minimum.
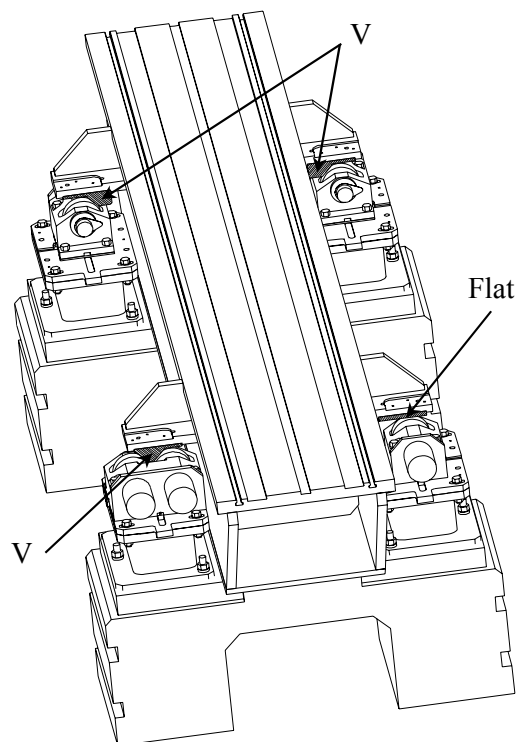

Fig. 5: Kinematic girder support: one flat +2 V seats balance the needed five DOFs (sway, heave, pitch, yaw and roll)—the surge, given its smaller relevance, was originally left to a simple strut system

In the final layout, the movers' kinematic chain on the driving side includes a simple and low-cost d.c. motor-worm gear assembly (Angst&Pfister type 0277 SW2K 404.004; nominal voltage: 24 VDC; reduction ratio: 1:78) and a planetary gearbox (Neugart type PLE 80; reduction ratio: 1:40). The arrangement allows a pseudo stepper motor with resolutions (defined as magnitudes of the smallest detectable motions) better than 2 μm to be obtained. The system was originally powered by pulse-width-modulated (PWM) motor power supplies.

The feedback signal of the achieved position is obtained using BFA series Baumer absolute rotary encoders (type BFA 0A.05Y4096/503463) mounted on the driven side of the kinematic chain; the readout of the movement of the cam is independent from backlashes on its driving side. The resolution of the feedback signal has been increased from 12 to 17 bits (corresponding to 0.00275° i.e., a displacement resolution of $\leq$ 0.25 μm) by in-house-developed IPM-900 interpolation module

interfaces based on SSI I/O units. The electronics can down-load the acquired data directly to the SLS control system through a VME output channel, integrating the girder positioning system fully into the SLS EPICS-based control system [16].

The adopted arrangement also allows the inclusion of motion bounding via precision Baumer Electric My-Com F75/S35 limit switches, and provides additional (i.e., redundant—the motion is already bounded by the design geometry of the eccentric cams as well as by software interlocks) security in the preservation of the integrity of the vacuum chamber.

3.3 Position-monitoring systems (HLS and HPS)

The necessity to continuously monitor the positioning stability of the girders, because of the long time deterioration of their initially aligned location, is met by using the hydrostatic levelling system (HLS) and the horizontal positioning system (HPS); both have micrometric-range accuracies (Fig. 6).
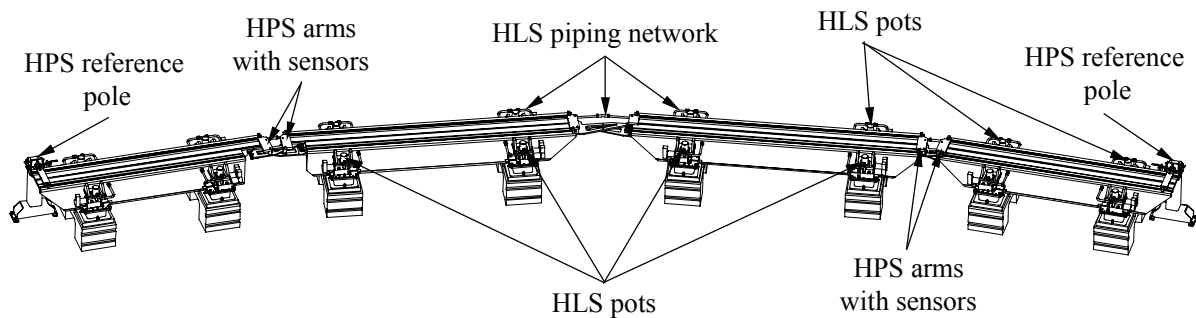

Fig. 6: A 30° sector of the SLS storage ring

The HLS consists of cylindrical stainless steel pots (ϕ = 10 cm) developed in collaboration with the Edi Meier & Partner AG company (Fig. 7). The pots are connected by a half-filled stainless steel pipe (outer diameter: 25 mm, inner diameter: 22 mm) around the ring; this configuration allows the problems associated with differential thermal expansion of the working fluid in different pots to be avoided. For easy of installation, localized Tygothane (radiation hardened poly-urethane) inserts are used, compensating for the small thermal and other misalignments of the piping network. With such an arrangement, a single reference altimetric level is obtained (Fig. 6).

Originally, de-mineralized water was the working fluid in the system since it has well-known properties, is easy to handle, and environmentally friendly and cheap.

The sensing elements are capacitive proximity gauge-based and linked to the SLS EPICS-based global control system. The non-contact measurement principle allows corrosion due to moistening or wetting of the contact points, as well as mineral deposits on the sensors, to be avoided. Moreover, the temperature of the sensor is kept above that of the water, avoiding condensation effects (which would cause corrosion and mineral deposits on the sensor); the temperature in each pot is constantly monitored to avoid temperature-induced apparent level changes (see, for example, Ref. [17]). The position of the sensors in the pots, as well as the dimensions of the pot itself, have been optimized to minimize the influence of the surface meniscus effect on the measurements and the capillary wall effects. An O-ring protects the electronics from corrosion. To keep wiring costs low, all the analog ($\pm$ 10 V) signals of one storage ring girder are multiplexed and digitized in a local HLS electronics. Each pot is equipped with a touch sensor; this feature allows a remote recalibration of the sensor by raising the water level up to it [18].

The resolution of the system is better than 2 μm, with the specified absolute accuracy and repeatability better than 10 μm. The maximum range of the sensors is 14 mm, while the range measurement used is $\pm$2.5 mm.

Four pots are installed on each girder (Fig. 6) allowing its vertical position (heave) as well as pitch and roll to be measured (in fact, three pots would be sufficient, with the fourth one giving

statistical data for increasing the precision, as well as covering possible failures). The pots are installed on the girder brackets so that both the ground movements and eventual differential dilatations of the girder supports can be taken into account. Each storage ring TBA (four girders) can be valved-off for maintenance purposes, thus lowering the settling times at refilling. The filling system restores the water level in the network after changes due to evaporation. The signals of the sensors next to the inner filling station are used to control the filling and emptying valves, respectively.
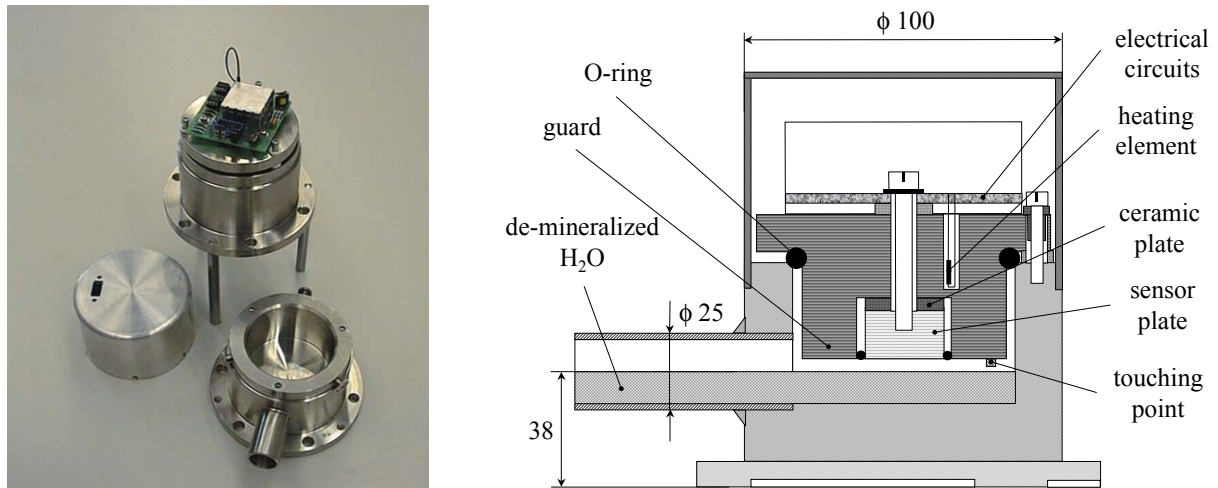

Fig. 7: The HLS pot (a) and the layout of its interior structure (b)

The horizontal positioning system (HPS) monitors horizontal girder movements and is constituted by pairs of lever arms under the girder surface equipped with optical encoders (Fig. 8). By extending the system in a 'train link' arrangement (Fig. 6), the relative horizontal displacements of adjacent girders can be correlated with respect to artificially created references (reference poles) at the beginning and at the end of each TBA (Fig. 9—there is no absolute reference as in the HLS). The position of the reference poles is determined by the accuracy of the conventional alignment methods, which is better than 100 µm.
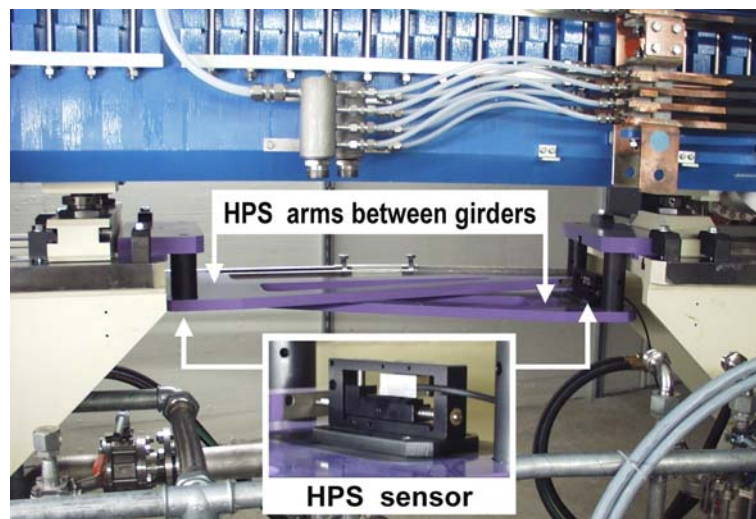

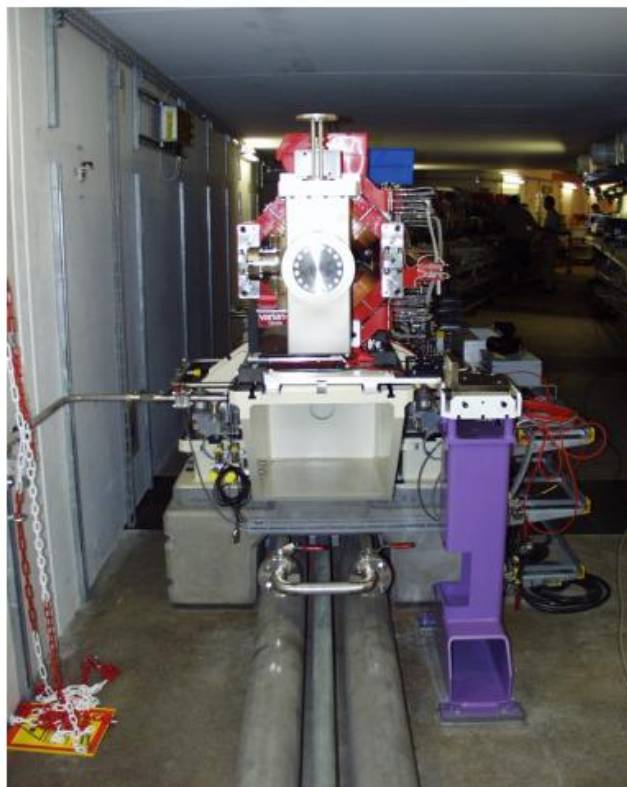**Fig. 8:** The HPS system mounted on girders

Fig. 9: An HPS reference pole

The four girders of a single TBA can be treated as either a self-contained system ('partial train link') or as part of the whole SLS storage ring ('full train link'). Using the artificial references as starting points, any motion of individual girders can be detected and traced back via a 2N dimensional linear system of equations—N being the number of girders taken into consideration in the calculation––with the girder transversal displacements (sways) and yaws as the unknowns. Since roll and pitch also affect the readouts of the HPS sensors, they have to be measured in advance via the HLS system [19].

The measuring sensor used for the HPS system is a Renishaw type RGH24Z50A00A absolute linear encoder with a 0.5 μm resolution and a working range of ± 2.5 mm; eight encoders are used in each TBA of the SLS storage ring. An in-house-developed encoder counter module (RHC 900) is employed to acquire the data, serialize them, and send them to the global SLS control system [20].

4   Beam-based alignment

For diagnostic purposes, it was envisaged that the SLS storage ring beam trajectory be measured using 72 high-precision BPMs [21] located between the magnets. Encoders similar to those used for the HPS system are then employed for monitoring the positions of the BPMs with respect to adjacent quadrupole magnets; the resulting readings are taken into account when the final electron-beam position is calculated. These data can be used to remotely align the girders using the mover system described, thus obtaining beam-based alignment. In fact, the girder mover system can be used like the corrector magnets to obtain closed-orbit and even coupling correction via the correction matrix, which correlates the BPM readings to the girder re-alignment motions needed (in the correction matrix, the girder misalignments are treated as correctors in the classical beam dynamics approach).

The beam-tracing simulations performed have shown that the static vertical closed-orbit corrections can be completely covered by girder alignment, while in the horizontal direction proper selection of the girders to be re-positioned via the movers allows the corrector magnet strength used to be reduced by a factor 4 (Fig. 10). This kind of alignment can take over most of the static orbit correction and leave the corrector strengths for the dynamic correction (active orbit feedback) and local bump creation for matching the beamline acceptances or for machine studies. Since beam-based girder alignment is a dynamic method and, in principle, may be done on-line with the stored beam, it appears to be a superior substitute for magnet sorting [19].
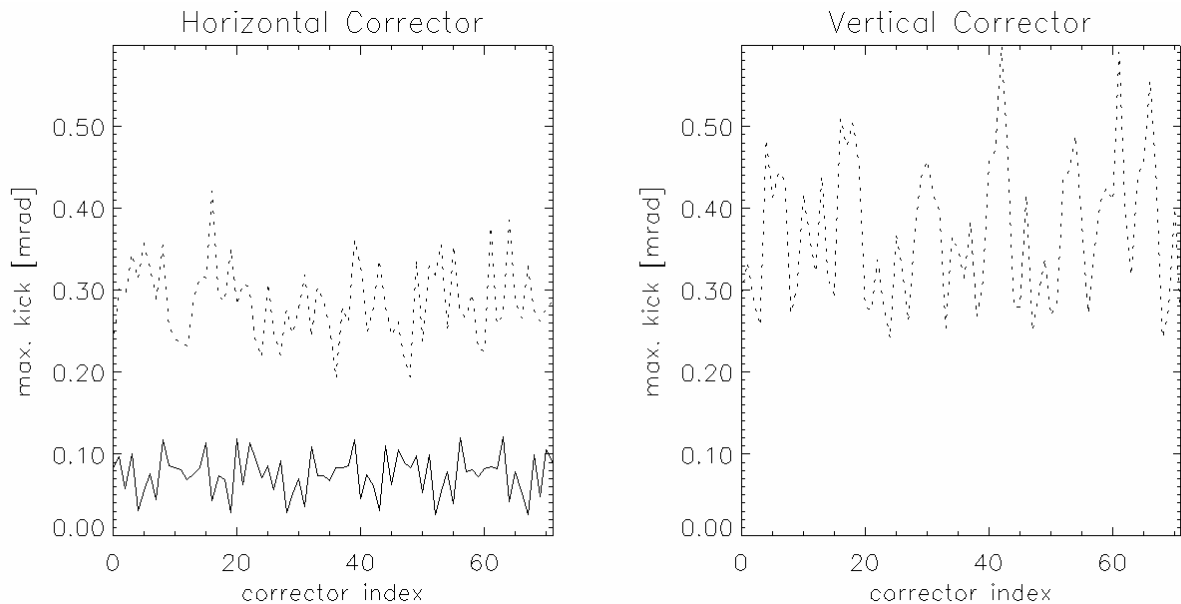

Fig. 10: Maxima of corrector magnet strengths before (dashed) and after (full line) closed-orbit correction through girder alignment. Two hundred random misalignment seeds were generated and corrected. The random errors assumed partial train links over four girders with r.m.s. (2σ cut) displacement errors of 300 μm for the (virtual) girder joints, 100 μm for the joint play (i.e. errors in the HPS and HLS readings), and 50 μm for magnets and BPMs positioning tolerances relative to the surfaces of the girders.

5 Tests on prototypes

5.1 Girder system

The delivery of the girder prototypes prompted an extensive design review and measurement campaign. In particular, the following tests have been carried out:

- The dimensional checks of the main components were carried out at the PSI laboratories via a Renishaw 3D coordinate measuring machine with micrometric range precisions. It was established that the design tolerances were met.

- The straightness accuracy of the reference surfaces was assessed using the HP 5529A Michelson-type heterodyne laser interferometric system. In the optical configuration used (Fig. 11), the measurement principle is based on an interferometer with a Wollaston prism. The prism is slid along the girder and has a different refractive index for each of the two polarized components of the laser beam; these are deviated by two equal and opposite angles towards a fixed retro-reflector. The reflector contains two plane mirrors that reflect the beam components back along their respective paths. The difference in optical paths of the two beam components is proportional

346

to the displacements perpendicular to the incoming beam, and the value of the girder surface quality (indicated with 'a' on Fig. 11) will be obtained simply by multiplying the interferometric measurement by a constant $(1/[2 \sin(\Phi/2)])$. In this case, given the range of measurement (4.5 m), the resolution of the optical set-up is 100 nm.

- The measurement system illustrated proved that the very tight tolerances ($\pm$ 15 μm) on the reference surfaces of the girders were met, and proved the deflection of the girders under the weight of the magnets to be smaller than 20 μm.

- The mounting and alignment procedures were reviewed. As a result, several alignment reference points have been added both to the mover supports and to the girder bodies. Also, the vertical and horizontal degrees of freedom have been completely decoupled, further contributing to the ease of the alignment procedure.
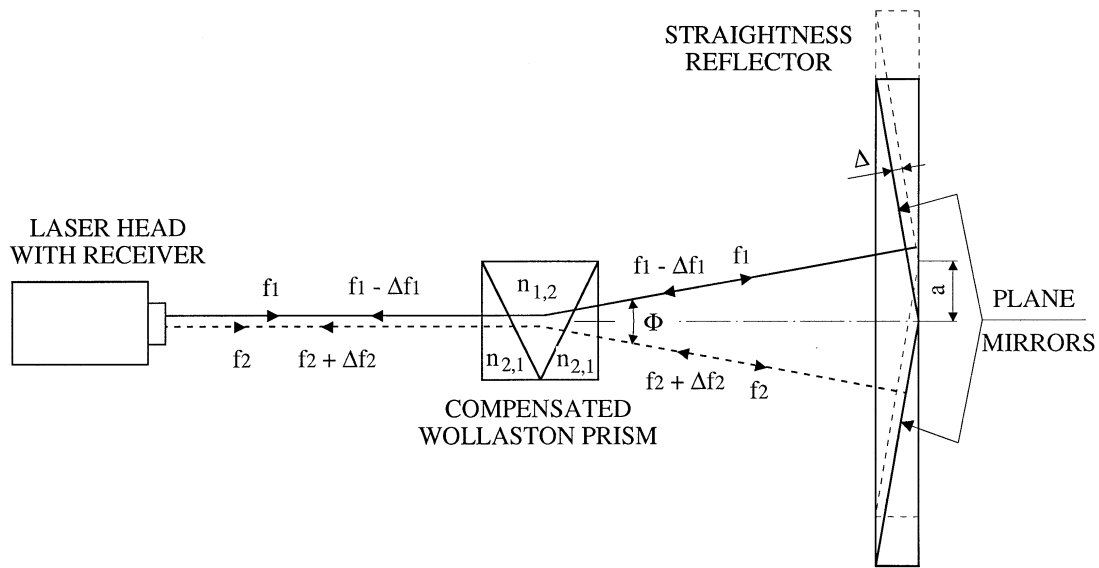

Fig. 11: Straightness measurement principle

5.2 Mover system

- The tests on the mover system proved its functionality.

- An 85 000 cycles fatigue test of the mover-to-girder interface under full load was performed. The electron microscopy analysis of the surfaces involved showed some fretting of the mover surface (Fig. 12), implying the need to change the material of the cam and increase its surface hardness to 60 HRC.

- The measured resolution and repeatability of a single mover proved to be better than the specified $\pm$2 μm while the resolution of the whole girder was within $\pm$ 3–5 μm. The positioning repeatability (also called precision, i.e., the range of deviations in the output position that occur for the same input command) of the system in the whole common working window proved to be better than the specified $\pm$10 μm, with the relative errors (difference between the (mean) actual component motion and its ideal motion) below 5% for 'small' range (up to 0.1 mm and 0.1 mrad) 5 DOF motions, and below 1% for bigger ones [22].

- Software allowing full operational control of the mover system, and creating all the pre-conditions for easy and reliable alignment of the SLS storage ring, when coupled with the diagnostics equipment, for beam-based girder alignment (see above), has been optimized [19] and tested proving its functionality. In fact, the geometric relations coupling the girder position to the

movers' angles of rotations are rather complex, and positioning requires a control unit to make the respective calculations.

- The development of this algorithm also allowed the simulation of girder behaviour. It was established that, when one misalignment at a time is compensated for, the mover working windows would cover a range of ±5–7 mm for linear motions and of ±5–7.5 mrad (±3.5–7 in the case of the 4.5 m long girder) for the angular ones, a combination of misalignments reduces these ranges to a common 5-dimensional region limited by one cubical and four hyper-hyper cubical regions, resulting in a common working window of ±1.4 mm for linear displacements and ±1–1.5 mrad for angular motions [19].

- Inverse software to calculate the girder displacements from the angles of the movers was developed to interpret the encoder feedback in metric units and check the convergence of the movements performed to the respective reference positions.

- The mover power supply and control systems, originally a self-standing unit, have been integrated into the global SLS EPICS-based control system.
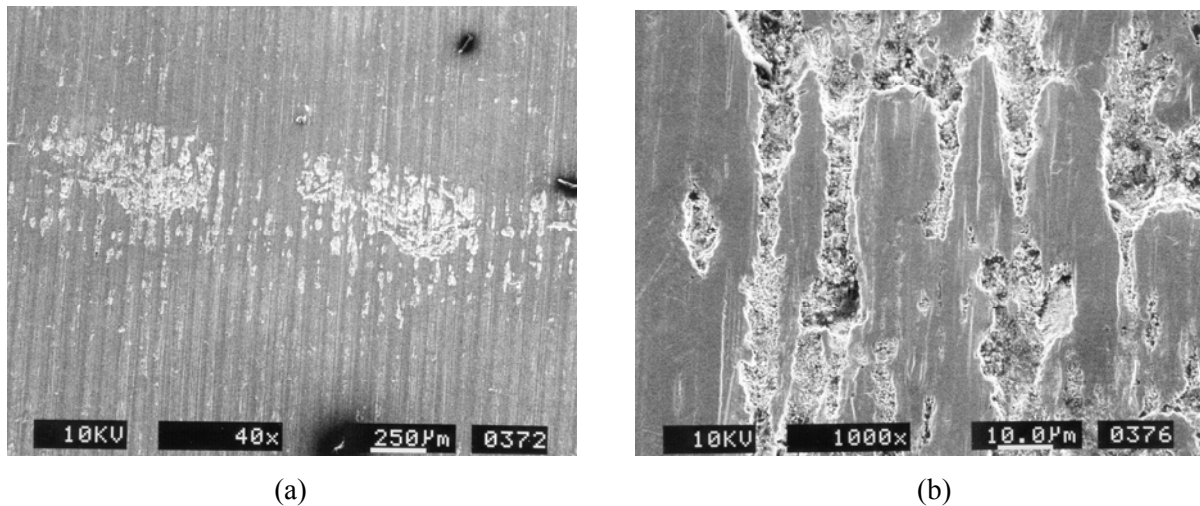

(a)   (b)

Fig. 12: Electron microscopy of the cam surface after the fatigue test: (a) 40 and (b) 1000 times magnification

5.3 Hydrostatic levelling system

The analog output of the HLS pots is a non-linear voltage signal. A suitable calibration procedure had to be developed for the pots readings, i.e., the determination of the correlation of the output voltage to the water level in the pots. Several pots were placed on a horizontal plate, whose planarity was checked via a high-precision inclinometer, and then connected by a tube. A reference pot, calibrated by observing the touching position of a micrometer device to its water surface, was used. The water level in the common piping network was then slowly raised while concurrently measuring the output voltage of the reference and the pots being calibrated. An automatic algorithm was employed to determine the calibration constants, i.e., to fit the measured output voltage of the pots being calibrated to the water level data of the reference pot. A third-order polynomial fit can then be used to correct the eventual non-linearities of the measurements; however, if the measurement range is kept reasonably small, the conversion formula can be simplified to [18]:

$$mm = \text{volt}^2 \cdot C_1 + \text{volt} \cdot C_2 + C_3 \qquad (1)$$

where C_1, C_2 and C_3 are the calibration constants being determined, and volt is the output signal of the pots.

Preliminary results obtained with a prototype installation of the HLS system onto the girders established that:

- The repeatability of the measurements for long range motions (/1 mm) is better than ±10 µm, while for motions limited to 100 µm it is better than ±3 µm. Given the mounting onto the girder, this measurement also included inaccuracies incurred through moving, which indicates that the repeatability of the HLS system itself is much better.

- The measurement on the girder installation also established that the settling times are very short after filling. In fact, a further measurement on a 100 m piping network (Fig. 13) with HLS pots mounted every 20 m, and with one pot mounted on a movable support (so that a precise vertical motion could be imposed on it), showed [23] that even with extreme perturbations the settling time for the attainment of the precision needed is shorter than that reported in previous installations [24] (Fig. 14).

- The stability of the measurements in both test set-ups proves the vibration influence on the measurements to be negligible, making unnecessary the mechanical (inserts to cut surface waviness and reduce waves) or software (scan of all or individual sensors with high data rates, with an application of FFT or spline fits to estimate undisturbed reference planes) vibration filtering, considered as a possible option.

- A test, heating one of the pots by ±2°C, performed on the same set-up in Fig. 13 indicated that the resulting difference in the readings was limited to ±1 µm, i.e., that the temperature effects have a small influence on the overall system stability [23]
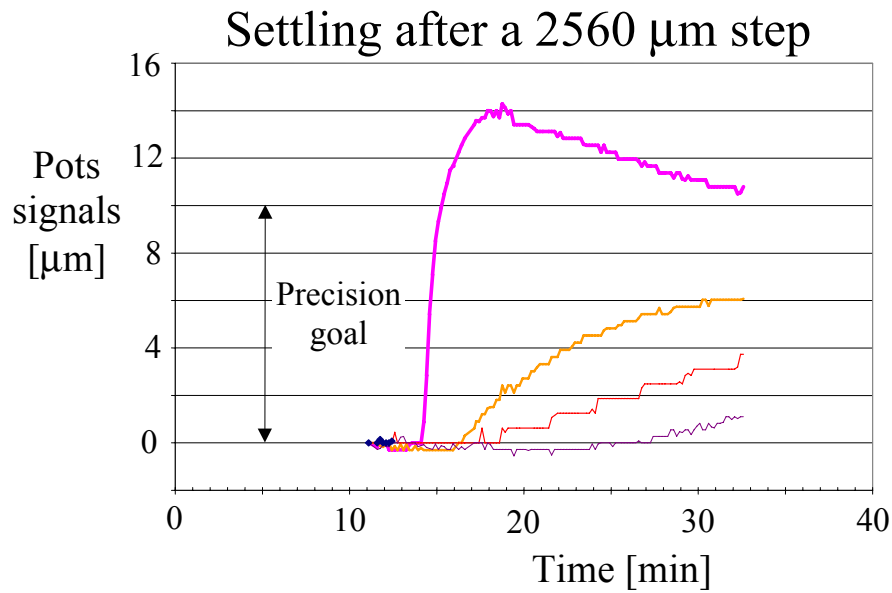

Fig. 13: A 100 m piping HLS experimental set-up

Fig. 14: Response of the pots in the experimental set-up to a 2.56 mm vertical motion of one pot

5.4 Horizontal positioning system

Preliminary tests were also performed on the prototypes of the HPS sensors mounted on girders (Fig. 15). Using laser interferometric measurements as a reference, it was established that the relative error of the HPS data does not exceed ±1 µm with a repeatability in the range of ±1 µm (Fig. 16), i.e., comparable to the resolution of the sensors.

Fig. 15: HPS prototype being validated with the laser interferometer
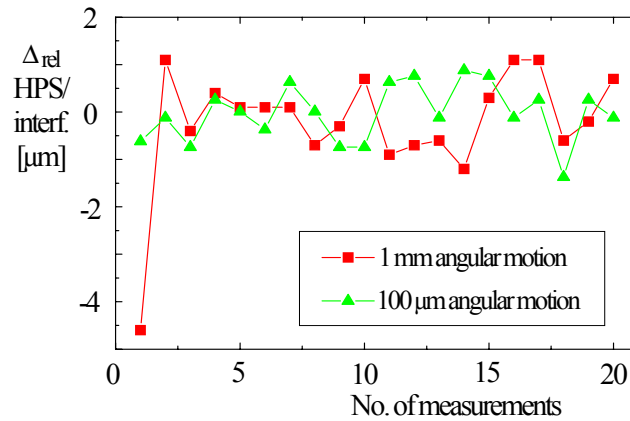
350

Fig. 16: Relative error between HPS sensors and the interferometric measurements for angular girder motions

6 Dynamic stability

Ground vibrations displace the magnetic elements and generate a time-dependent closed-orbit distortion. Experiments at the SLS require a highly stabilized photon beam spot in the frequency range below 100 Hz to reduce the residual r.m.s beam jitter to 10% of the electron beam sigmas. Assuming an emittance coupling of 1% and the r.m.s. optics amplification factor of ~ 8 horizontally and ~ 5 vertically (Fig. 17 as already mentioned, shows how mounting several magnets onto a girder generates a far smaller amplification than would occurr for individually supported quadrupoles) [25], this translates into the mechanical vibration amplitudes of 0.2 μm in the vertical and of 2 μm in the horizontal direction. Thus, a realistic estimate of the emittance growth needs the vibration transmissibility of the girder/magnet assemblies to be established.
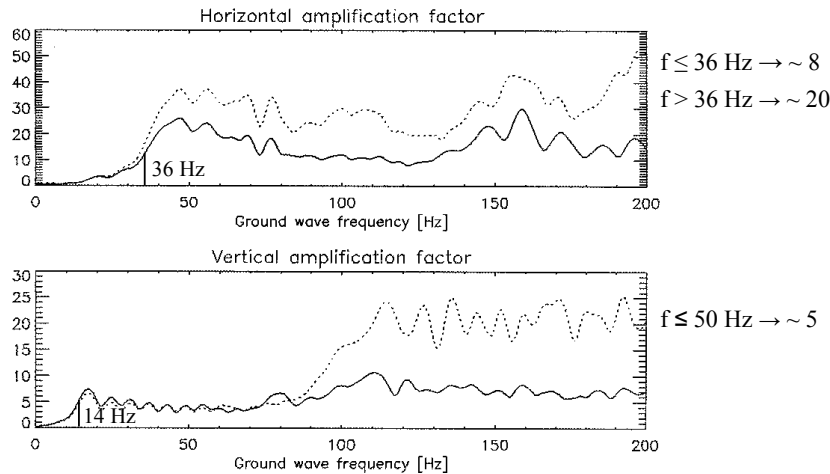

Fig. 17: Simulated optics amplification factors for the SLS machine (full line: elements on girders; dashed: single elements). An increase of the amplification factors at the indicated betatron wavelengths is observed (assumed velocity of sound in the soil: 500 m/s) [25].

The first step in this direction was to evaluate the incoming ground noise spectrum, where the micro-seismic events, such as those caused by ocean waves (e.g. the '7 seconds hum' at 0.14 Hz), could be neglected, since their wavelengths (several kilometres range) are too big to influence the behaviour of the SLS complex (the wavelengths are far greater than the betatron wavelength of the SLS machine).

- A first measurement of the spectrum at the SLS site in spring 1997 indicated that, because of the neighbouring road and the equipment installed at the PSI premises (especially a nearby

351

compressor working at a 12.3 Hz frequency), significant excitations could be induced in the frequency range below 40 Hz. In fact, under 'natural' excitations, amplitudes of up to 20 nm in the vertical and 40 nm in the horizontal direction were measured, while under 'random' events, such as weights dropped from a crane, and explosions in a nearby quarry, the maximum measured amplitudes went up to 100 or more.

- In a second phase (end 1998), a thorough vibration measurement campaign was performed on the girder prototypes checking the influence of the number of contact points and of the type of the concrete pedestal-to-metal support interface. For this purpose, the system was excited in the frequency range of man-induced vibrations (traffic, machinery, in the 10–50 Hz region) by an eccentric mass driven by a d.c. motor (Fig. 18). The results obtained with PCB Piezotronics (USA) ICP accelerometers were analysed using the corresponding mono-dimensional analytical model. Once an estimate of the stiffness and damping of the system was obtained, the transmissibility of the excitation from the ground to the system was assessed considering the theory of the vibration response of a mechanical system to the vibrations of its basement. It was thus established that, although there are some resonance peaks in the frequency range considered (mostly in the horizontal direction), the transmissibility of the system is such (< 10) that the amplitudes of the vibrations under 'natural' excitations should remain in the acceptable range.

- Based on the experimental results, the parameters of the numerical (FEM, Fig. 19) model mentioned were tuned, enabling further design variables (screw types at the concrete-to-metal interface, grouting of the supports, ribs in the girder body) to be investigated. It was proved that, from a dynamic point of view, the system configuration with a kinematic support arrangement, grouted supports, and with a proper fixing of the magnets onto the girder body efficiently fulfils the design goals.

- In summer 1999, measurement of the new SLS building indicated the ground motion amplitudes under natural excitations to be below 10 nm.

- In spring 2000, a vibration measurement campaign established the dynamic response of the girder system under the natural excitation coming from the ground floor in the storage ring tunnel (Fig. 20) under real operating conditions. These included the operation of the cooling and conditioning units, the crane unit, machinery in the experimental area, i.e. all equipment that could introduce additional excitation. At this stage, a thorough measurement campaign of a girder excited by an impulse hammer also allowed its eigenfrequencies and mode shapes to be accurately determined. This provided evidence that the transmissibility of the girder/magnet assembly existed [10], while its dynamics were greatly influenced by the dipoles on its ends (and the 'cross-talk' between neighbourhood girders) see Fig. 21. Some significant girder eigenfrequencies in the range of excitations produced by the technical devices, which are present at and around the SLS premises, have been found—especially in the 25–40 Hz range. Nevertheless, the resulting amplitudes were, in the worst case-scenario, still in the 10–30 nm range, and hence an order of magnitude below those needed to produce significant perturbations of the storage ring performances.

- In the horizontal direction, more relaxed tolerances have been given lower relevance, the vibration amplitudes of the girder assemblies are higher than those in the vertical plane, but still an order of magnitude lower than that required (Fig. 22).

- Subsequent measurements of the SLS building vibrations at various locations have clearly confirmed the very quiet conditions for the machine and the experimental floor. The vibration amplitude levels are such that the building would be suitable for tunnel electron microscopy (TEM) and scanning electron microscopy (SEM) equipment. What is clearly visible, however, is the influence of the crane, which raises the vibration amplitudes in the entire lower frequency range. On the other hand, the influence of the infrastructure equipment is negligible.
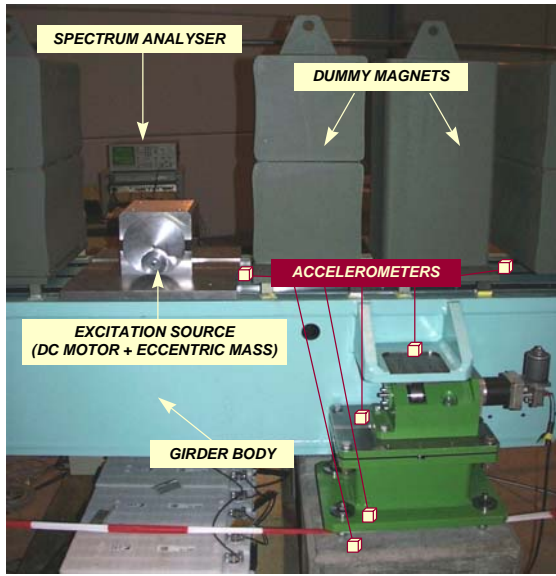
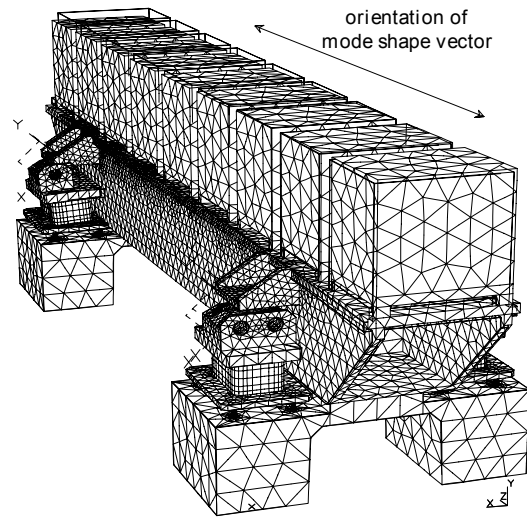**Fig. 18:** Experimental set-up for vibration measurements

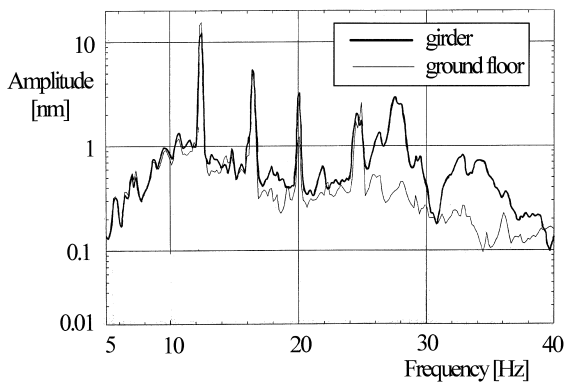**Fig. 19:** FEM modal model of the girder system

Fig. 20: Spectrum of the storage ring tunnel floor and of the girder/magnet assembly under natural excitation – vertical plane
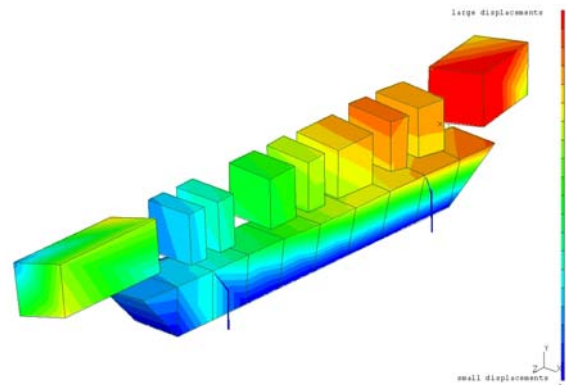

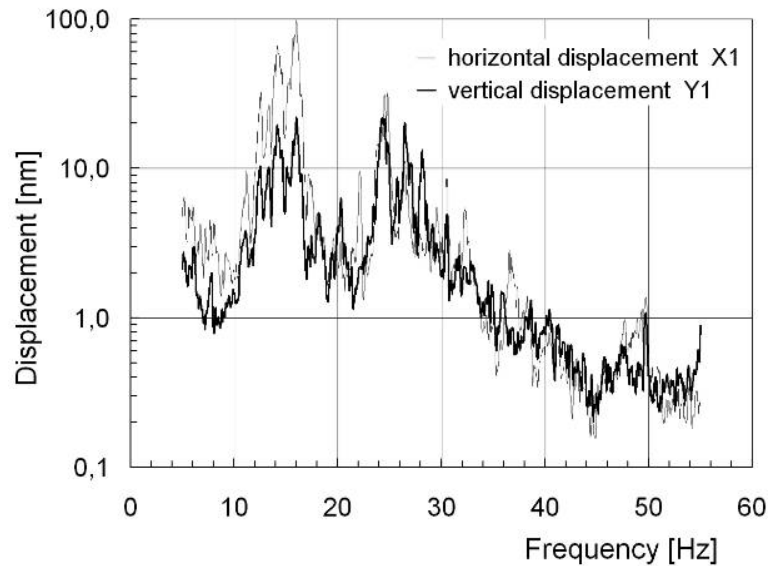**Fig. 21:** Eigenmode of the girder/magnets assembly evidencing the influence of the dipoles on the dynamic response

353

Fig. 22: Vibration amplitudes on the dipoles in the horizontal and vertical planes with the active cooling water circulation (worst case)

7 Installation in the storage ring

Based on the above tests, the design of the SLS storage ring support, alignment, and disturbances compensation systems was optimized and approval for serial production of the various components was given. During the production cycles, quality control was very thorough. Particular attention was dedicated to the reference surfaces of the girders, measured with the HP laser interferometric system (Fig. 23); where needed, the reference surfaces were re-ground to meet the required tolerances (±15 μm). The inspection records accompanying every girder and the respective components have been obtained from the Swedish manufacturer Olssons Mekaniska. Considered necessary, a double check of the tolerances achieved was performed on the critical components at the PSI premises. All the girder and mover pieces were delivered to PSI on or before schedule.
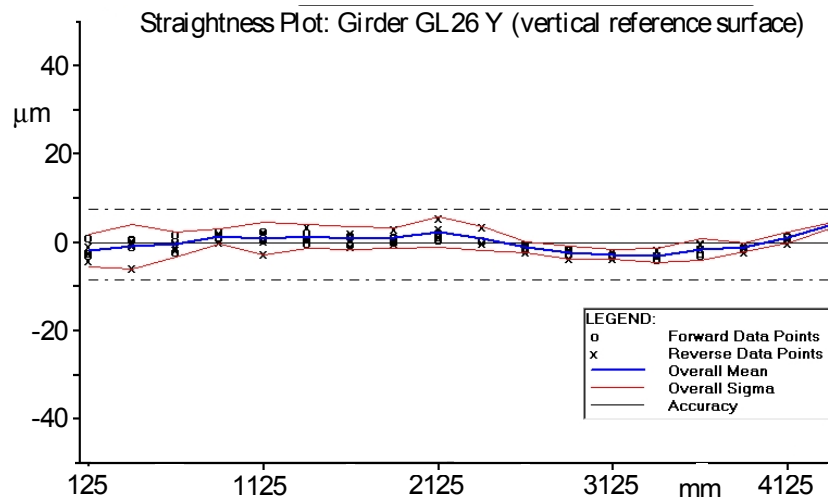

Fig. 23: Typical results obtained by measuring the straightness of the girder reference surfaces

The assembly of the motor-gearbox units and encoders (delivered by Mueller Konstruktionen AG and Eltromatic AG) onto the movers was completed in early November 1999, as was the determination of the movers' zero positions (which had to be performed with micrometric accuracy to

allow for the proper usage of the respective software—the tools needed were developed in-house). The steel girder pedestals were concurrently mounted and grouted onto the concrete blocks, and then the movers were mounted onto the pedestals thus enabling cabling of the respective d.c. motors and of the encoders.

Towards the end of 1999 magnet delivery began. The storage ring magnets comprise 36 dipoles and 174 quadrupoles for bending and focusing, and 120 sextupoles for chromaticity correction (72 of the sextupoles have additional horizontal and vertical dipole windings for closed-orbit correction).

In each TBA there are two 0.8 m long magnets, each providing 8° of bend, and one 1.4 m long magnet bending the trajectory by 14°; the dipoles were manufactured by Tesla Engineering. Each was measured with a Hall array magnetic measurement bench showing a small spread between the magnets of each type; a full field map of a few dipoles was also obtained and used to calibrate the series measurements and the 3-D field model of the magnets [26].

The multipoles were manufactured at the Budker Institute of Nuclear Physics (BINP), Russia. Stringent requirements were placed on the location of the magnetic axes, as well as on the field quality. Each magnet was measured on a rotating coil magnetic measurement bench. After the initial measurement, the magnet pedestals were machined to bring the magnetic axe positions within the specified tolerance of ± 30 µm. After delivery to PSI, the multipoles were re-measured following the same procedure [26], see Fig. 24.

Fig. 24: BINP specialist at the SLS rotating coil magnetic measurement bench

After completion of the magnetic measurements, the magnets were mounted onto the girders and the first TBA was installed in the SLS storage ring on 9 December 1999 using a specially designed lifting tool (Fig. 25).

Fig. 25: Mounting of the first girder/magnet assembly onto its place in the SLS storage ring

The network-based pre-alignment of the girder/magnet assemblies was carried out using the Leica Geosystems LTD500 laser tracker [27] (the SLS storage ring tunnel has 155 network reference points).

The upper parts of the yokes were removed, and the first 18 m stainless steel vacuum chambers, corresponding to one storage ring TBA or girder sector, were installed (Fig. 26). The chambers have an antechamber and contain discrete water-cooled copper absorbers to intercept most of the synchrotron radiation not transmitted to the beamlines (as the main source of gas load, the absorbers are positioned close to the pumps). It is worth noting that the vacuum chamber pieces that form one sector were initially vacuum fired up to 950°C at CERN and DESY. The vacuum sectors (including diagnostic elements and lumped pumps) with gate valves at both ends were assembled in the clean room on the SLS experimental hall, and finally baked-out for roughly a week at 250°C. No in situ bake-out and no bellows are used in the vacuum sectors (for impedance reduction reasons). For details about the SLS vacuum system refer to Ref. [28].

Fig. 26: Vacuum chamber transport from the bake-out oven to the storage ring tunnel

The installation of all the storage ring girder/magnet assemblies (including the respective water and electrical connections) and the vacuum chambers was completed in early summer 2000. In parallel to mounting the TBAs, mounting, assembly, as well as cabling and piping of the elements of the girder position monitoring systems (HPS, HLS) were carried out. To comply with safety requirements, all the HLS, HPS cabling and mover systems were completed with halogen-free cables (Fig. 27).

For the HLS, whose development was considered critical given its innovative design, a LabView-based control unit was installed in the technical gallery proving its functionality; an Oracle database to download the data acquired and its storage into the global SLS control system was successfully completed. The installation of the automatic filling station allowed the on-line filling procedure to be tested and optimized. A new series of tests was performed in the SLS storage ring. The results, obtained compared to laser-tracker and mover-encoder measurements, showed that the HLS allows reliable micrometric accuracy data with relative errors in the 1% range to be achieved. The only drawback was the relatively long settling time needed to achieve the correct readings on the heave, since in this case the water contained in the HLS pots of the moved girders has to flow in/out from the whole storage ring. In the case of pitch and roll motions, the water is basically redistributed only in the pots of the moved girder, limiting the settling times to a range of a few minutes [29].

Fig. 27: View of the SLS tunnel after installation of the storage ring elements

8 Operational experience

8.1 Girder and mover system

During the final alignment phase of the storage ring it was clear that the strut-based longitudinal girder fastening originally foreseen did not allow the desired positioning accuracies to be attained and maintained as a result of the breakage of frictional contacts. New roller bearing-based, backlash-free fastenings were developed and mounted in a very short time. These allow simple and repeatable positioning of the 9 ton girder-magnet assemblies on the micrometric scale.

A further problem encountered during alignment was electrical noise generated in the mover cables by the PWM motor power supplies adopted. This hindered the proper functionality of movers

furthest from the mover electronics. Stabilized d.c. Kepco Bipolar Operational Power Supplies/Amplifiers BOP 36-6M (±36 V, ±6 A) have since been adopted, efficiently solving the problem.

With these two minor modifications to the original arrangement, the final alignment of the SLS storage ring allowed the positioning of whole TBAs (4 girders with up to 28 magnets mounted onto them) with micrometric accuracies within 1 to 2 days. The beam-based measurements performed during machine commissioning allowed the achievement of the required machining (girder and magnet total tolerances within ±50 μm) as well as alignment tolerances to be confirmed. In fact, SLS is probably one of the very few synchrotron radiation facilities where the very first turn of the electron beam in the storage ring was achieved with all the correctors turned off [30].

8.2   Horizontal positioning system (HPS)

The HPS has worked reliably ever since it was commissioned, allowing the correlation of beam current temperature stability in the storage ring tunnel with respect to beam stability to be assessed [31].

8.3   Hydrostatic levelling system (HLS)

Despite the excellent commissioning results cited above, the HLS readings showed millimetre range drifts on several pots after a few weeks of operation with longer time scales (Fig. 28). Some of these drifts have been traced back to poor fixing and alignment of the piping network which, with the rather high water level in the pipes at the time, led to the creation of Bernoulli tube effects (monitoring of local pressure differences between the created tube sections). However, even when additional supports were added (especially at the interface between the HLS pots and the pipes—Fig. 29), considerably improving the alignment of the piping network, the problems encountered, which were completely randomly distributed in space and time, persisted.
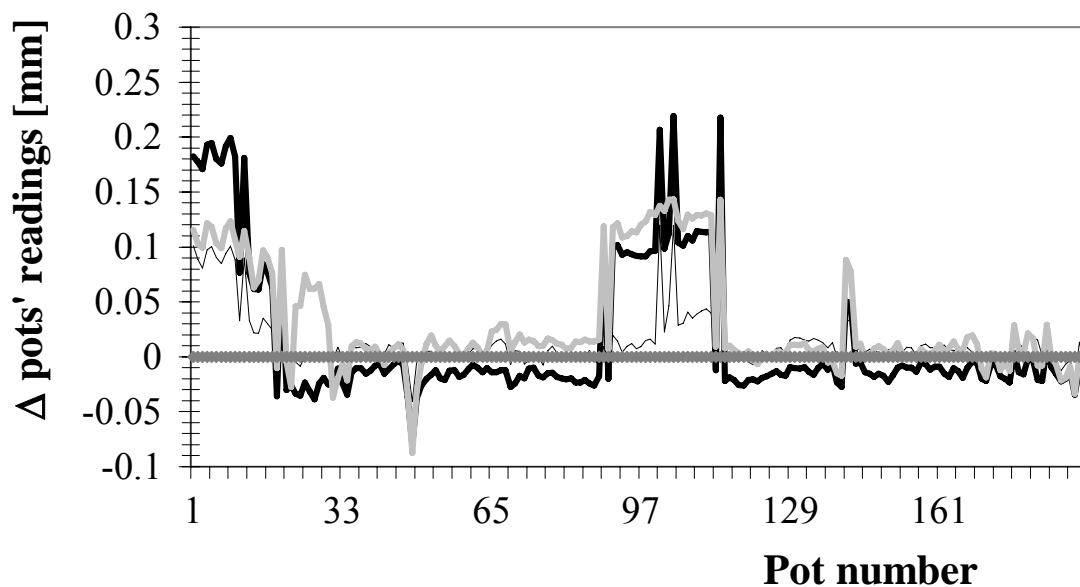

Fig. 28: Relative change of the readings on all pots of the SLS storage ring during three weeks in spring 2001

Fig. 29: Additional piping fastenings at the HLS pots

It was assumed that the phenomena observed were due to the formation of a foggy layer above the water level, which could influence the respective dielectric constant. A thorough study of the theoretical aspects of the air-water mixtures has excluded this as the possible cause of the problem.

A humidity build-up at the guard-to-sensor interface of the HLS pots, inducing a parasitic capacitance, was thus postulated. Changing the material of the insulator plate with glass, quartz and different types of ceramics and inducing electronic compensation of the drifts, proved unsuccessful. Only the introduction of an O-ring between the guard and the sensor plate (hindering the humidity path to the upper parts of the pot) led to stable readings within ±10 μm over several weeks. After a few months, however, roughly half of the pots started drifting again [32].

After several attempts to tackle this problem (with very large time constants needed to attain any meaningful results) [32], a satisfactory solution was eventually obtained by adding 30% of an antibacterial fluid and alcohol solution to the HLS working fluid. Seemingly, this has killed the my-cells of the fungi observed under a microscope on the surfaces of the sensors and the guards [Fig. 30(a)], which could have been creating 'water channels' that induced the parasitic capacitances observed [18]. This theory cannot explain all the phenomena observed.

Nevertheless, since the adoption of the fungicide (January 2002), the HLS readings are stable to a point at which the Earth's tides can be observed. The normal environmental variations in the SLS machine tunnel induce effects limited to 2–3 μm on the behaviour of the system. Regular shutdowns, opening of the storage ring tunnel roof to install new equipment, and human presence in the tunnel do introduce larger perturbations [Fig. 30(b)].

The recent full integration of the HLS into the SLS EPICS-based control system will now allow the study of any residual 'parasitic' effects, as well as the correspondence of the HLS readings with long-term survey data.
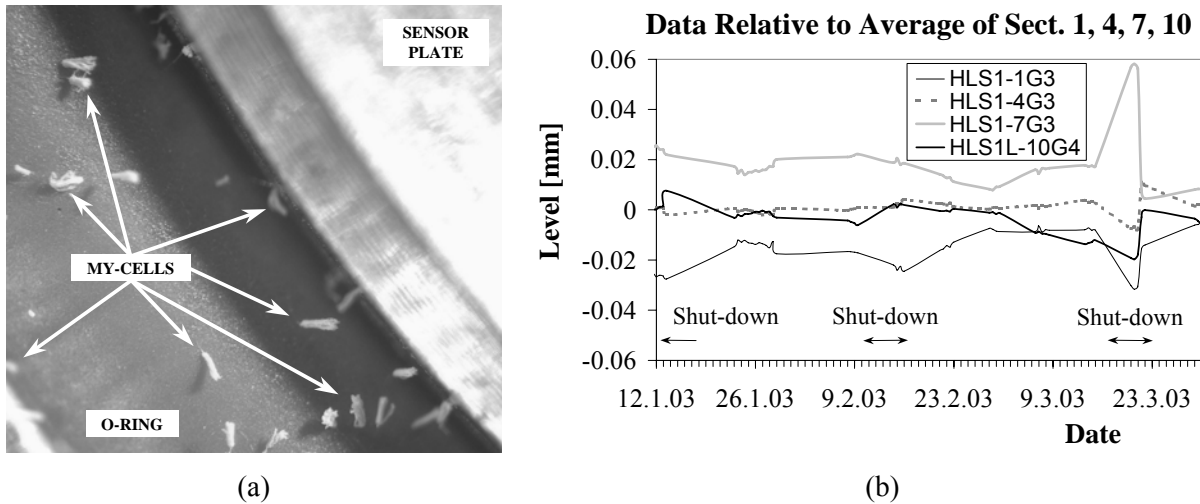
Fig. 30: My-cells observed on the HLS pots (a) and the results obtained after the adoption of a fungicide (b)

8.4   Dynamic stability

Beam-based measurements performed using the digital BPMs mentioned confirmed the girder eigenfrequency shown above and corresponding vibration amplitude measurements [33]. Furthermore, a vibration measurement campaign performed at the end of 2002 as part of a CERN PhD thesis confirmed the data (Fig. 31). Thanks to the low transmissibility of the girder structures (< 10 in the vertical and < 20 in the horizontal direction), the installation of new beamline equipment, including several additional excitation sources, did not induce any meaningful perturbations to the storage ring optics or to the photon beam [34].
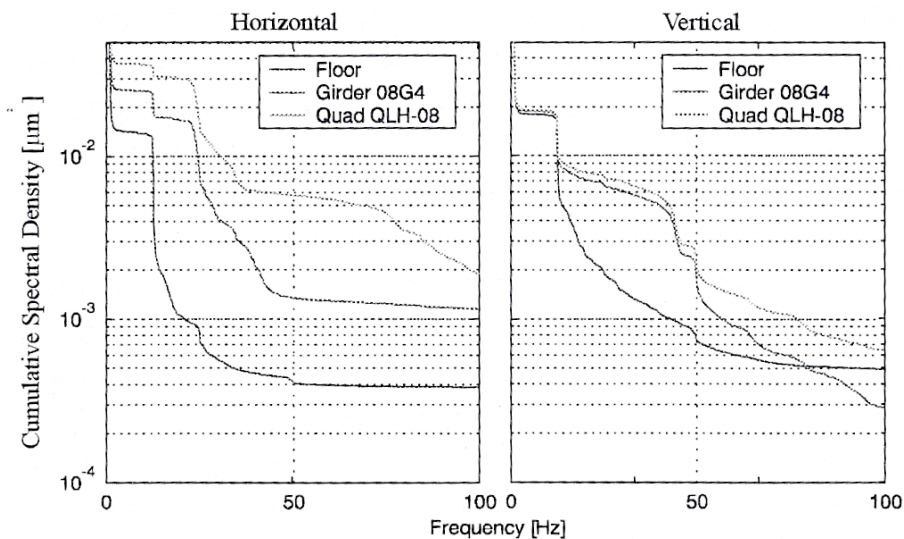

Fig. 31: Vibration amplitudes on the storage ring elements obtained late 2002

9   Conclusions

Although some minor upgrades have been necessary, the SLS storage ring support, positioning and position monitoring systems, optimized by thorough analytical, numerical, and experimental assessments, have been successfully installed and commissioned, allowing a significant reduction of the alignment time spans to be obtained. The system's effective and sophisticated design has so far given excellent results at the SLS. This has led to the creation of all the preconditions for beam-based storage ring dynamic alignment (allowing the potential optimized use of the corrector magnet) when

linked to the diagnostics data. The design is further validated by the high degree of interest shown by other synchrotron radiation facilities (SLAC, DIAMOND, CLS, SOLEIL, APS, ELISA, etc.) to adopt similar solutions.

In the end, it is important to note that the role of mechanical engineering at the synchrotron light sources extends much further than storage-ring support, positioning, and position monitoring systems [35]. In the case of the SLS project, the Mechanical Engineering Group had to design several beamline components or whole beamlines (e.g., diagnostic beamline X05DA), organize the design, production and follow-up of several critical machines (e.g., third harmonic superconducting RF system), insertion device (including in-vacuum devices) and beamline components (the first set of four SLS insertion devices and beamlines had very active involvement of the SLS Mechanical Engineering) outsourced to external companies. In this process, the group has mastered the skills to deal with complex tasks, such as:

- advanced design of ultra-high vacuum (UHV) and radiation compatible, high-heat load and high-precision equipment and instrumentation;

- analytical and numerical modelling of structural (static and dynamic, as well as modal), thermal, non-linear (buckling, contact, large displacements), and transient problems;

- experimental techniques such as the Michelson-type heterodyne laser interferometric measurements mentioned in the linear (resolution down to 10 nm), angular (resolution: $0.05''$) and straightness (resolution: 10 nm) optical configurations, as well as vibration measurements on machine and beamline (including optical) components;

- a key competence, original approaches to the analytical modelling and experimental assessment of the performances of UHV-compatible, ultra-high precision devices.

Such skills are proving to be very valuable in the upgrades of the machine (e.g., the femto-second project) as well as for the development of new SLS beamlines.

Although the role of 'non-physics' (vacuum, alignment, mechanical, electrical) experts in the development of new synchrotron radiation facilities is sometimes underrated, all of the above clearly proves that such complex projects require an interdisciplinary approach, where the expertise of all the personnel involved is of vital importance.

Acknowledgements

References

[1]   Proc. 1st Int. Workshop Mech. Eng. Des. SR Equip. Instr. (MEDSI 2000), Villigen, 2000.

[2]   Proc. 2nd Int. Workshop Mech. Eng. Des. SR Equip. Instr. (MEDSI 2002), Argonne, 2002.

[3]   Proc. 3rd Int. Workshop Mech. Eng. Des. SR Equip. Instr. (MEDSI 2004), Grenoble, 2004.

[4]   G. Margaritondo, Experiments with synchrotron radiation: basic facts and challenges for accelerator science, these Proceedings.

[5]   P. Elleaume, Present limits and future developments of storage ring synchrotron sources, Proc. 8th Int. Conf. SR Instr. (SRI 03), San Francisco, 2003.

[6]   C. J. Bocchetta, Beam quality and lifetime, these Proceedings.

[7] C. J. Bocchetta, Closed orbit stability, these Proceedings.

[8] A. Streun, Lattices and emittances, these Proceedings.

[9] A. F. Wrulich, Proc. 1999 Part. Accel. Conf. (PAC 99), New York, 1999, p. 192.

[10] M. Böge, Paul Scherrer Institut Sci. Rep. 1998, Vol. VII, 1999, p. 15.

[11] R. E. Ruland, Proc. 4th Int. Workshop Accel. Align., Tsukuba, 1995, p. II/233.

[12] J. Brnic, Nauka o cvrstoci, University of Rijeka, Rijeka, 1991.

[13] M. Böge *et al.*, Proc. 6th Eur. Accel. Conf. (EPAC 98), Vol. 1, Stockholm, 1998, p. 644.

[14] G. Bowden *et al.*, SLAC-PUB-95-61326132, 1995.

[15] A. H. Slocum and A. Donmez A., *Prec. Eng.* **10** No. 3 (1988) 115.

[16] R. Kramert, Girder Mover Encoder Readout - Technical Specification, PSI Publ., 2000.

[17] D. Roux, Proc. 1st Int. Workshop Accel. Align., Stanford, 1989, p. 37.

[18] E. Meier *et al.*, Hydrostatic Levelling System – Service Guide, E. Meier & Partner, Switzerland 2002.

[19] A. Streun, Swiss Light Source-TME-TA-2000-0152, 2000.

[20] V. Schlott, Paul Scherrer Institut Sci. Rep. 1998, Vol. VII, 1999, p. 19.

[21] V. Schlott, Paul Scherrer Institut Sci. Rep. 1999, Vol. VII, 2000, p. 25.

[22] P. Wiegand, Swiss Light Source-TME-TA-2000-0145, 2000.

[23] E. Meier, Messresultate 100 m Test, E. Meier & Partner, 2000.

[24] D. Roux, A New Alignment Design - Application of ESRF Storage Ring, ESRF Publ.

[25] M. Böge *et al.*, Proc. 1999 Part. Accel. Conf. (PAC 99), New York, 1999, p. 1542.

[26] L. Rivkin, Paul Scherrer Institut Sci. Rep. 1999, Vol. VII, 2000, p. 13.

[27] F. Q. Wei *et al.*, Paul Scherrer Institut Sci. Rep. 1999, Vol. VII, 2000, p. 30.

[28] L. Schulz, Vacuum aspects, these Proceedings.

[29] S. Zelenika *et al.*, Paul Scherrer Institut Sci. Rep. 2000, Vol. VII, 2001, p. 30.

[30] A. Streun, Paul Scherrer Institut Sci. Rep. 2000, Vol. VII, 2001, p. 12.

[31] V. Schlott, Paul Scherrer Institut Sci. Rep. 2001, Vol. VII, 2002, p. 28.

[32] S. Zelenika, Paul Scherrer Institut Sci. Rep. 2001, Vol. VII, 2002, p. 30.

[33] V. Schlott *et al.*, Proc. 2001 Part. Accel. Conf. (PAC 01), Chicago, 2001, p. 2397.

[34] J. Krempansky and M. Dehler, Paul Scherrer Institut Sci. Rep. 2002, Vol. VI, 2003, p. 38.

[35] S. Zelenika *et al.*, Mechanical engineering at the Swiss Light Source, 3rd SLS Users' Meeting, Villigen, Switzerland, 2002.